

# Phase-separation during sedimentation of dilute bacterial suspensions

Bryan O. Torres Maldonado, K. L. Galloway, Quentin Brosseau, and Paulo E. Arratia

Department of Mechanical Engineering & Applied Mechanics, University of Pennsylvania, Philadelphia, PA 19104. E-mail: parratia@seas.upenn.edu

Numerous natural systems showcase the sedimentation of passive particles in presence of swimming microorganisms. Here, we investigate the dynamics of the sedimentation of spherical colloids at various *E. coli* concentration within the dilute regime. Results show the appearance of two sedimentation fronts, a spherical particle front and a bacteria front. We find that the sedimentation speed of passive particles decreases as bacteria concentration ( $\phi_b$ ) is increased. As  $\phi_b$  is increased further, the sedimentation speed becomes independent of  $\phi_b$ . The timescale of the second front captures the behaviour of both regimes, and a simple model based on particle-bacteria interactions is proposed that can describe this timescale for a range of  $\phi_b$ . Remarkably, all experiments collapse onto a single master line by using the second front timescale. A phenomenological model is proposed that captures the sedimentation of passive particles in active fluids.

## 1 Introduction

The settling of particles in the presence of microorganisms is a ubiquitous natural process<sup>1-6</sup>. Sedimentation of biological matter, for instance, plays an important role on the distribution of plankton in oceans, which is key part of the carbon cycle (i.e. ocean's biological pump) that transports carbon from the ocean's surface to depth<sup>7-9</sup>. From a technological stand point, microbial activity can affect many process such as the production of food, biofuels, and even vaccines<sup>10-14</sup>. While there is a rich history (and much still to understand) on the subject of sedimentation of passive suspensions<sup>15-20</sup>, there has been a growing interest on systems that emulates the sedimentation of natural processes, particularly those that include living matter such as swimming bacteria<sup>21-26</sup>. An important feature of such active systems is that particles (living or synthetic) can inject energy and drive the fluid out of equilibrium even in the absence of external forcing<sup>27</sup>. This leads to many unusual phenomena, including low values of reduced viscosity<sup>28,29</sup> and enhancement in particle diffusivity<sup>30-34</sup>. The effects of activity on the sedimentation of passive particles, however, remain poorly understood.

Past studies have explored the *steady-state* sedimentation of active particle suspensions<sup>21,22,24-26</sup>. Experiments with active (phoretic) colloidal suspension in stationary state found that density profiles decay exponentially with height yielding a sedimentation length that is larger than expected for thermal equilibrium<sup>21,24</sup>. Phoretic Janus particles tended to aggregate and behave as adhesive disks<sup>24</sup> and show polarization<sup>26</sup>. Similar results are found even when the sedimentation speed is of the same order as the particle propulsion speed<sup>26</sup>; slower exponential decay with increasing bacterial activity is described by using an effective temperature (or diffusivity) that correlates with the particle's ability to self-propel and achieve larger diffusivities than from thermal fluctuations alone. Experimental results agree relatively well with theory<sup>35,36</sup> and simulations<sup>25,26,37,38</sup> for active particles that are either non-interacting<sup>35,36</sup> or with limited hydrodynamic interactions<sup>37,38</sup>.

Sedimentation experiments with live organisms have been far less common and show unusual phenomena. For example, bacteria has been shown to enhance sedimentation rates in the presence of polymers due to aggregation<sup>39</sup>. In mixtures of swimming algae and passive particles, the (exponential) steady-state sedimentation profile of passive particle is found to be described by an effective diffusivity (or temperature) that increases linearly with the con-

centration of swimming microbes<sup>40</sup>. Recently it was found that the sedimentation speed of passive particles can be significantly hindered by the presence of swimming microorganisms (*E. coli*) in the dilute regime<sup>23</sup>; the hindered settling function for these settling active suspensions is captured by a Richardson-Zaki-type equation<sup>41</sup> with an exponent that is both much larger than for passive systems and is a function of bacteria activity. The *time-dependent* concentration profiles can be adequately described by an advection-diffusion equation coupled with bacteria population dynamics, and with a dispersivity parameter that increases linearly with bacteria concentration<sup>23</sup>. Despite these recent developments, the effects of particle-bacteria interactions on particle sedimentation process is still not well understood.

Here, we experimentally investigate the sedimentation dynamics of dilute active suspensions using mixtures of passive colloidal spheres and swimming *E. coli*. These initially well-mixed suspensions settle for a period up to 3 days (depending on bacterial concentration) and image analysis techniques are used to track the height of the sedimentation front. Our results shows that the sedimentation speed of passive particles decreases as bacteria concentration ( $\phi_b$ ) is increased. As  $\phi_b$  is increased further, the sedimentation speed becomes independent of  $\phi_b$ . The two species, bacteria and particles, phase-separate into two distinct sedimentation fronts at a critical time  $t_c$  that is a function of the species diffusivities and settling speeds. A simple model based on particle-bacteria interactions is proposed that can describe particle settling fronts in the presence of bacterial activity for a range of  $\phi_b$ .

## 2 Experimental Methods

Experiments are prepared by mixing *Escherichia coli* (wild-type K12 MG1655) and polystyrene spheres (density  $\rho = 1.05 \text{ g/cm}^3$ , Thermo Scientific) with a diameter  $d$  of  $2 \mu\text{m}$  in deionized (DI) water. Bacteria are grown to saturation ( $10^9$  cells/mL) in culture media (LB broth, Sigma-Aldrich). Both spheres and the saturated culture are centrifuged (Centrifuge 5430, eppendorf) and mixed with DI water to reach the desired bacterial volume fraction.

In this paper we experimentally study sedimentation of particles in the presence of bacteria. We use two experimental methods: optical measurements of settling speed and measurements of diffusivity of particles and bacteria, both dead and alive. Diffusivity is measured from samples taken throughout the sedimentation process to asses changes with time, such as loss of bacteria motility. Specifics of our diffusivity experiments have been reported previously in Ref.<sup>23</sup>. There are also some details presented here in the Supplemental section. In the sedimentation experiments, we transfer 1.5 mL of the prepared suspensions into glass vials (9.7 mm

<sup>0</sup>Department of Mechanical Engineering & Applied Mechanics, University of Pennsylvania, Philadelphia, PA 19104. E-mail: parratia@seas.upenn.edu

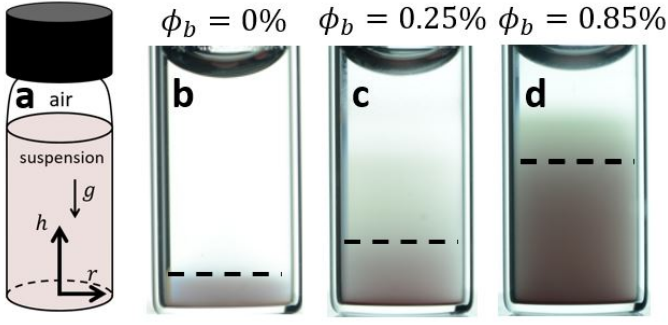


**Figure 1** Experimental setup and sample images are shown from left to right: (a) A schematic of the setup and bacteria/particle suspensions. Passive particles are  $2 \mu\text{m}$  polystyrene spheres, subject to gravity; volume fraction  $\phi_p = 0.04\%$  kept constant for all experiments. Swimming activity is provided by *E. coli*, a  $2 \mu\text{m}$  rod shaped bacterium. Sample snapshots of sedimentation experiments with (b) only passive particles ( $\phi_p = 0.04\%$ ), and mixture of passive particles with *E. coli* (c) at  $\phi_b = 0.25\%$  and (d)  $\phi_b = 0.85\%$ . All vials samples are shown at time  $t = 40\text{hr}$ . Note the appearance of two sedimentation fronts, bacteria and particle, in (c) and (d).

in diameter, 20 mm in height), as shown schematically in Fig. 1a. The suspensions are homogenized by hand with a pipette so that the bacteria and colloids are uniformly distributed at the start of the experiment. These vials are placed in a water tank to maintain the vials at room temperature  $T_0 = 22 \text{ }^\circ\text{C}$  and remove optical aberrations during imaging; cylindrical vials are preferred to avoid effects from sharp edges. Images are taken every 10 minutes for a period of 2-3 days with a Nikon D7100 camera that is equipped with a 105 mm Sigma lens. The light source is a Edge-lit Collimated Backlights (CX, Advanced Illumination).

In our experiments, the initial bacteria volume fraction  $\phi_b$  in the vials is varied from  $0.15\% \leq \phi_b \leq 0.95\%$ , while the spherical colloids volume fraction is kept constant at  $\phi_p = 0.04\%$ . Both  $\phi_b$  and  $\phi_p$  concentrations are considered dilute, and no large scale collective behavior are observed on the prepared bacteria-particle suspensions. The range of  $\phi_b$  used here are below which collective motion is generally observed ( $\approx 10^{10}$  cells/mL)<sup>42</sup>. Under these dilute conditions, *E. coli* swims at speeds ranging from  $10 \mu\text{m/s}$  to  $20 \mu\text{m/s}$  by the actuation of a helical flagellar bundle. This mode of swimming, under steady conditions, can be described in the far field by an extensile dipole flow (i.e., "pusher")<sup>43</sup>.

### 3 Results and Discussion

Sample snapshots of the sedimentation experiments are shown in Fig. 1(b-d) at  $t = 40$  hours. The control passive case (no bacteria,  $\phi_b = 0$ ) is shown in Fig. 1b, while  $\phi_b = 0.25\%$  and  $\phi_b = 0.85\%$  cases are shown in Fig. 1c and Fig. 1d, respectively. Note that  $\phi_p = 0.04\%$  is kept constant for all experiments shown here. The images show that bacterial activity significantly hinder the settling speed of passive particles. We find that the passive particle sedimentation front sits higher in the  $\phi_b = 0.25\%$  case than in the no-bacteria case. This trend continues for the  $\phi_b = 0.85\%$  case, which indicates that particle settling speed decreases with increasing  $\phi_b$ . We also observe the formation of two sedimentation fronts, one for the passive particle and one for the bacteria, as shown in Fig. 1(c-d). These two fronts settle with different speeds.

While the appearance of a bacteria front has been previously discussed<sup>23</sup>, here we will focus on quantifying and understanding the appearance of the two sedimentation fronts and its relationship to

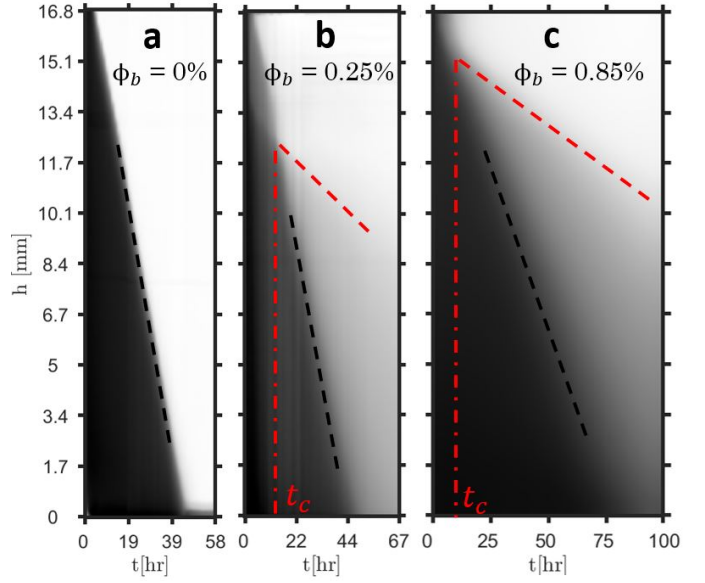


**Figure 2** Kymographs for sedimentation at fixed particle concentration ( $\phi_p = 0.04\%$ ) and different bacterial concentration. From left to right: with no bacteria ( $\phi_b = 0\%$ ),  $\phi_b = 0.25\%$ , and  $\phi_b = 0.85\%$ . Two fronts are seen when  $\phi_b \geq 0.15\%$

particle sedimentation front speed. As a first measurement, we obtained the settling speed of live bacteria, which is the speed of the second front,  $V_{l,b} = 0.02 \pm 0.002 \mu\text{m/s}$ . We performed an additional sedimentation experiment of spherical particles in presence of inactive bacteria (dead), and found that bacteria settling speed is  $V_{d,b} = 0.04 \pm 0.002 \mu\text{m/s}$ , which is important below.

We begin by measuring the sedimentation height of the passive spheres front as a function of  $\phi_b$ . The sedimentation height ( $h$ ) of the front is located in the vial by identifying the peak in the vertical gradient of the image intensity. By plotting  $h$  as a function of time ( $t$ ), we can extract a front sedimentation speed  $V_s$  and define a hindered settling function  $H(\phi_b)$  as a function of bacterial concentration. The hindered settling function is defined by the ratio of the mean sedimentation speed  $V_s$  over the sedimentation speed of a single particle (also known as Stokes settling speed) such that  $H(\phi_b) = V_s(\phi_b)/V_0$ . The sedimentation speed of a single polystyrene colloid  $V_0$  in a viscous fluid of viscosity  $\mu$  in absence of inertia is calculated by the force balance between the gravitational force and viscous drag acting on the particle. This yields  $V_0 = \Delta\rho g d^2 / 18\mu$ , where  $\Delta\rho$  is the density difference between the colloid and the suspending liquid,  $g$  is the acceleration due to gravity ( $g = 9.81 \text{ m/s}^2$ ),  $\mu$  is the fluid viscosity, and  $d$  is the particle diameter. For the  $2 \mu\text{m}$  polystyrene particles in water, the sedimentation speed  $V_0$  is  $0.12 \mu\text{m/s}$ .

Figure 2(a-c) shows sedimentation kymographs ( $h$  vs  $t$ ) for the passive ( $\phi_b = 0$ ) case and two active suspensions,  $\phi_b = 0.25\%$  and  $\phi_b = 0.85\%$ . These experimental kymographs are obtained by the juxtaposition of a single pixel line at the center of the vial for each image of the time series. As noted before, all samples have a fixed particle volume fraction ( $\phi_p = 0.04\%$ ). In each case a sedimentation front is formed, and moves downward from the top of the container at a speed  $V_s$ . A first look at the corresponding kymographs reveal that the velocity  $V_s$ , here visible as the slope of the colloid front (black dashed line), decreases as the concentration of bacteria increases. We again observe the formation of a second front that appears after a critical time  $t_c$  (red dashed line). The

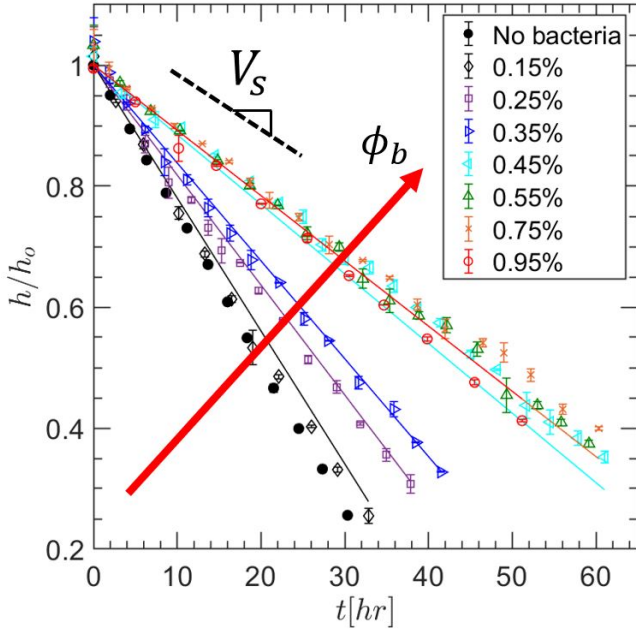


**Figure 3** Height of particle sedimentation front,  $h(t)/h_0$ , where  $h_0$  is the initial height tracked on the sedimentation process as a function of time for a range of bacterial volume fractions  $\phi_b$ . Data (open symbols) shows the decrease in front speed with an increase of bacterial volume fraction  $\phi_b$ . At higher bacterial volume fraction ( $\phi_b > 0.40\%$ ), bacteria no longer affects the sedimentation of passive particles. Solid lines are obtained by solving Equation 2. Solution to the equation as shown in Equation 4, captures relatively well the height of the front of passive particles for a wide range of bacterial concentrations  $\phi_b$ .

timescale  $t_c$  is defined as the time that the second front appears and diverge from the main sedimentation front. We immediately observed that the time of separation of the second front is a function of bacteria volume fraction, that is  $t_c = t_c(\phi_b)$ . Later in the manuscript, we will describe in detail the evolution of the fronts and propose mechanisms underlying their dynamics.

These kymographs allow us to determine the passive colloids sedimentation front position (or height  $h$ ) for the passive and active cases as a function of time. The front sedimentation speed  $V_s$  is then found by linear fits  $h(t) = -V_s t + h_0$ , where  $h_0$  is the initial front position; in all cases studied here, this linear relationship works relatively well even at long times ( $>24$  hours). In absence of bacteria ( $\phi_b = 0$ ), the front sedimentation speed  $V_s = 0.11 \mu\text{m/s}$ , which is relatively close to the sedimentation speed of a single sphere,  $V_0 = 0.12 \mu\text{m/s}$ . This result indicates that hydrodynamic interaction among passive particles are relatively weak in our study. This not surprising since particle volume fraction is quite dilute,  $\phi_p = 0.04\%$ .

The settling front of the passive colloids is characterized from the motion of the suspension interface as shown in the kymographs (Fig. 2). The height of the particle sedimentation front as a function of time for different bacteria volume fractions  $\phi_b$  is then normalized by the initial height  $h_0$ . The settling height of the front is linear through all experiments, so it is described by a average speed,  $V_s$  (Fig. 3). Results shows that the presence of bacteria hinders the sedimentation speed of the spherical colloids when compared to colloids settling under gravity without bacteria. A constant sedimentation speed is not a trivial result because the decrease in bacteria activity is commensurable with the time of the experiment. At 48 hours of experiment, 70 percent of the pop-

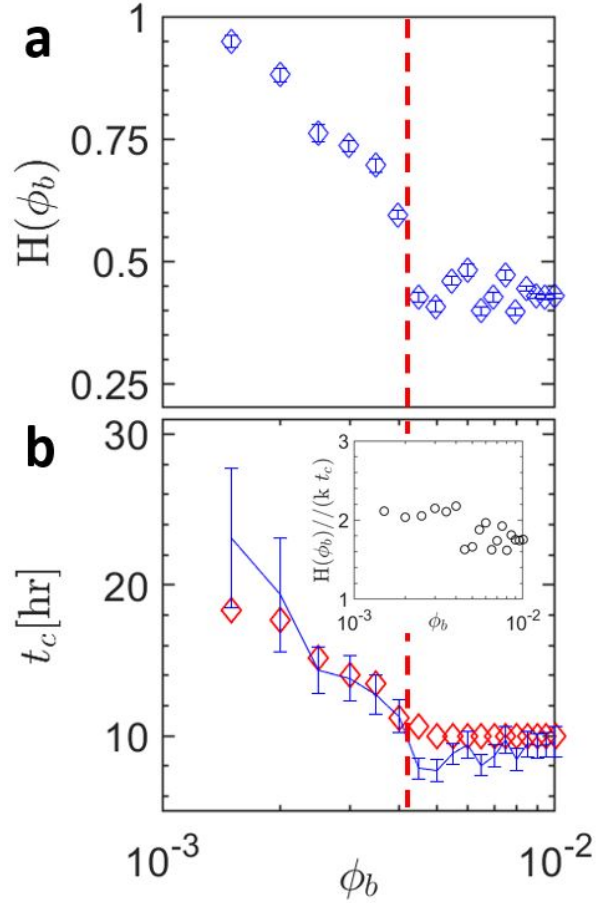


**Figure 4** (a) Hindered settling function  $H(\phi_b)$  as a function of bacterial volume fraction  $\phi_b$ . Two regimes are observed, a regime that is  $\phi_b$  dependent at low bacteria concentration ( $\phi_b \leq 0.40\%$ ) and a regime that is independent of  $\phi_b$  at higher bacteria concentration ( $\phi_b > 0.40\%$ ). (b) Time-scale  $t_c$  as a function of bacterial volume fraction  $\phi_b$ . Solid line shown in blue is the time-scale prediction obtained by Equation 1, which captures relatively well the experimental  $t_c$  for a wide range of bacterial concentrations  $\phi_b$  in the dilute regime ( $\phi_b \leq 1.0\%$ ). These results also shows that the time-scale  $t_c$  follows the same trend as  $H(\phi_b)$ . Inset plot is the ratio of the hindered settling function  $H(\phi_b)$  to the time-scale  $t_c$  and motility loss rate  $k = 6 \times 10^{-6} / \text{s}$ .

ulation has lost motility and behave as a passive colloid<sup>23</sup>. This has been previously characterized by a bacteria motility loss rate  $k$ , which is approximately  $6 \times 10^{-6} / \text{s}$  (see<sup>23</sup> and also SM for more information). The decrease in activity promotes a faster sedimentation; concurrently, the increase in passive particles (non-motile bacteria) should decrease the overall sedimentation speed. These two processes are not necessarily of the same magnitude.

Figure 3 shows, with increasing concentrations of live bacteria, the settling speed slows. Strikingly, this slowing of settling speed saturates when  $\phi_b > 0.40\%$ . This implies that the activity introduced via the swimming of bacteria slows the sedimentation of the particle front. However, at a much higher bacteria concentration, there is no longer an effect, indicating a transition. Because the introduction of swimming bacteria affects the settling of particles via their hydrodynamic interactions, we next investigate how the hindered settling function changes with increasing bacteria concentrations. A well-known method of characterizing the settling rate of passive particle systems is by computing the suspension hindered settling function  $H(\phi_b) = V_s(\phi_b)/V_0$ , where  $V_0$  is the set-

ting speed of a single particle and  $V_s$  is the suspension settling speed as a function of bacteria concentration,  $\phi_b$ . Here we explore this variable as a touchstone to previous literature and as a tool to develop our phenomenological model for the sedimentation of active suspensions. As shown in Fig. 4a, we find two main regimes for the quantity  $H(\phi_b)$ : (i) it initially decreases as  $\phi_b$  is increased up to ( $\phi_b \leq 0.4\%$ ) and (ii) it becomes independent of  $\phi_b$  as bacteria concentration is increased beyond 0.4%. As with Fig. 3, the hindered settling function reflects that the presence of bacteria slows particle sedimentation, but only up to a critical bacteria concentration ( $\phi_b = 0.40\%$ ). Figure 4b show similar trends for the quantity  $t_c$ , which is the time at which the second (bacterial) sedimentation front becomes visible; more on this below. The mechanisms for the appearance of this  $\phi_b$ -independent regime in the hindered settling function  $H$  (and  $t_c$ ) are unclear. We conjecture that any given particle is increasingly likely to be influenced by a bacteria within its vicinity as there are more bacteria. With enough bacteria, each particle is influenced and the effect saturates. This (saturated) regime exists, however, without involving a change in the bacterial dynamics such as collective motion that emergence at volume fraction  $\phi_b > 1\%$ <sup>42</sup>. In order to test this conjecture, we next quantify how frequently a bacteria and particle are expected to encounter each other to capture this transition based on the hydrodynamic interactions between particles and bacteria.

Both particles and bacteria are subjected to diffusion. At the microscopic scale, diffusion is achieved by Brownian motion of individual particles/bacteria. However, with the inclusion of an overall directional bias of each individual particle or bacteria, via swimming or gravity, a suspension gains a much richer set of behaviors, as outlined in the introduction. The ratio of diffusion and the square of forward velocity is a statistical quantification of how long it takes on average for one particle to interact with another. We calculate this ratio as:

$$t_c = \frac{6(D_{eff_b} + D_{eff_p} + 2(D_{eff_b}D_{eff_p})^{1/2})}{(V_0 - \Delta V)^2}. \quad (1)$$

where  $D_{eff_b}$  and  $D_{eff_p}$  are the diffusivities of bacteria and particles,  $V_0$  is the settling speed of a single particle, and  $\Delta V = V_s - V_b$  is the difference in velocities of particles and bacteria within the suspension. Notice that each of these quantities is measurable according to the methods outlined in the experiments section. As shown in Fig. 4b, we find that the critical time to contact,  $t_c$ , has a qualitatively similar form to the hindered settling function suggesting a deeper underlying relationship at play.

Note that Eq. 1 can be derived phenomenologically as follows. Let the distance travelled to contact be  $X_b + X_p$ , where  $X_b$  and  $X_p$  are the distances traveled by a bacteria and a particle respectively. We take this distance to be equal to the velocity difference multiplied by the time to contact:  $X_b + X_p = (V_0 - \Delta V)t_c$ . Now we note the definition of diffusivity as:  $t = X^2/6D$ , where the factor of six in the denominator represents three-dimensions. By assembling and solving for  $t_c$ , Eq. 1 is recovered. Next, we revisit the meaning of the critical time at the macroscopic scale.

As shown in Fig. 2(b-c) and Fig. 4b, the time when the second front appears changes with the initial bacteria concentration  $\phi_b$ . By investigating this time as a function of  $\phi_b$ , we observe that it is surprisingly similar to the  $t_c$  derived above (Fig. 4b). Recall the particles settling without bacteria do so faster than when bacteria are included and that a suspension of only bacteria will sediment more slowly than if particles are present. This means that a separation is inevitable in the two species suspension; i.e. particles push down bacteria and bacteria give buoyancy to the particles via their

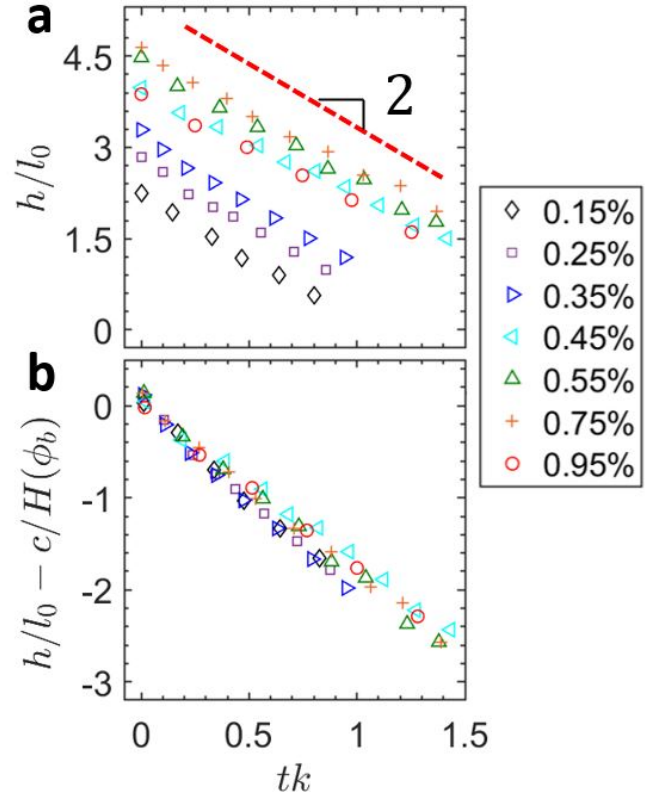


**Figure 5** (a) Normalized height  $h/l_0$  as a function of normalized time  $tk$ . Length-scale  $l_0$  is defined as  $l_0 = V_0 t_c$  where  $V_0$  is the sedimentation speed of a single sphere and  $t_c$  is defined as the escape time (initial time of second front). The timescale  $k$  is a constant motility loss rate of bacteria  $k = 6 \times 10^{-6}/s$ . Normalized plot shows a constant slope on all experiments, the slope as a value of  $1.97 \pm 0.050$ . (b) Normalized height as a function of the normalized time. The height was initially normalized by the length-scale  $l_0$ , and the time by the motility loss rate  $k$ . This normalization gave a constant slope of  $1.97 \pm 0.050$  as shown in (a). Now, the normalized height is shifted by a constant  $C$  divided by the hindered settling function  $H(\phi_b)$ . The shift on the normalized height made that all the experimental data with different  $\phi_b$  would collapse into a single line. The constant has a value of  $C = 1.955 \pm 0.045$ .

interactions quantified above. The finding here Fig. 4b suggests that the time it takes for bacteria to emerge from the particles is related to the time it takes for them to interact. This observation offers a direct link between the microscopic and the macroscopic dynamics of an active-passive suspension, which we will use below in determining a governing equation for height versus time.

All values shown in Equation 1 are measured from the sedimentation experiment and an auxiliary diffusivity experiment (see SI and Ref.<sup>23</sup> for more details). To characterize  $t_c$  as a function of bacteria concentration ( $\phi_b$ ), we evaluate the effective diffusivity of bacteria as  $D_{eff_b}(t = t_c) = D_{eff_b}(t = 0) e^{-kt_c}$ . Similarly, the effective diffusivity of particles in presence of bacteria is evaluated as  $D_{eff_p}(t = t_c) = D_{eff_p}(t = 0) e^{-kt_c}$ . Here we assume that the settling speed  $V_b$  of the bacteria that interact directly with the spherical particles change due to the large period of time that takes to separate from the particles in the low bacteria regime ( $0.15\% \leq \phi_b \leq 0.40\%$ ). Therefore, for the low bacteria regime we assume the following expression  $V_b = V_{d,b} - V_{l,b} e^{-kt_c}$ . Equation 1 captures relatively well the measurements of the timescale  $t_c$  (Fig. 4b). Across a wide range in  $\phi_b$  the experimental measure-

ments of  $t_c$  (red diamonds in Fig. 4b) are predicted within error by the predictions of Eq. 1 (blue line in Fig. 4b).

Next, we non-dimensionalize both sedimentation height of the front and time using the two time scales discussed above:  $t_c$  and  $k$  (Fig. 5a). Because the time-scale  $t_c$  captures the behavior of the two regimes observed in the hindered settling function data we use it to normalize height with  $l_0 = t_c V_0$ . We non-dimensionalize time by the motility loss rate,  $k$ . This yields an average slope of  $-1.97 \pm 0.050$  through all performed experiments (Fig. 5a).

We finally account for the intercept in (Fig. 5a) by noticing that it changes similarly to the inverse of the hindered settling function,  $H(\phi_b)$ . Therefore, we subtract the re-scaled height ( $h/l_0$ ) with a constant  $C$  divided by the hindered settling function  $H(\phi_b)$ . The constant  $C$  is obtained by equaling the intercept of  $h/l_0$  with  $c/H(\phi_b)$ , giving a value of  $1.955 \pm 0.045$ . Remarkably, all experiments collapse onto a single master curve (Fig. 5b). Putting together these experimental observations, the sedimentation front of passive particles can be described with the following differential equation:

$$\frac{h(t)}{t_c V_0} - C \frac{V_0}{dh/dt} = -2kt, \quad (2)$$

which can be rearranged to be

$$\frac{dh(t)}{dt} \left( \frac{h(t)}{t_c V_0} + 2kt \right) = CV_0. \quad (3)$$

We take the linear solution to this equation to obtain

$$h(t) = -2kt_c V_0 t + \frac{CV_0}{2k}. \quad (4)$$

Equation 2 shows that the sedimentation front of the passive particles are described by three main terms. The first term is height normalized by a diffusion based length scale associated with bacteria-particle interaction. The second term quantifies passive settling under gravity via the hindered settling function. The third term is the current time normalized by the motility decay rate. We note that a solution to Equation 2 is a line and is shown in Equation 4. If we solve the equation and revisit front height over time (Fig. 3), we observe that the solution captures all cases of bacterial concentration.

Our experimental observations show that sedimentation and separation of passive particle and bacteria suspensions is governed by bacteria-particles interaction. The injection of energy by the bacteria swimming motion plays an important role in the sedimentation process; its decay is quantified by a motility loss rate  $k$ . Crucially, separation occurs over very long length scales compared to mixtures of passive particles that have two different masses and is reminiscent of the effects of centrifuging. This effect saturates above a critical bacterial concentration ( $\phi_b = 0.40\%$ ). When saturated, bacteria no longer plays a role due to the active interactions and particles will be hindered due to increase of particle increase instead of the increase of activity.

Preparation of new experiments that track spherical particles while they sediment would help to understand these observations. This could be achieved by using a confocal microscope with a smaller vial. The downside of this proposed approach is that controlling the temperature at long times is a challenge. With this approach we would be able to obtain 3-D imaging as a function of time, which would provide the opportunity to track the spherical particles.

## 4 Conclusions

The sedimentation of passive particles in the presence of swimming bacteria is experimentally investigated. We find that bacterial activity (even in the dilute regime) hinders the sedimentation of passive particles and promotes the appearance of a second sedimentation front at a time  $t_c$ . Particle hindered settling function,  $H(\phi_b)$ , as well as  $t_c$ , show two distinct regimes: (i) a monotonic decay by increasing  $\phi_b$  and (ii) a regime in which both  $H(\phi_b)$  and  $t_c$  are no longer dependent of  $\phi_b$ . The timescale  $t_c$  is a function of the species diffusivities and settling speed, and a simple model based on particle-bacteria interactions is proposed that describes this timescale for a range of  $\phi_b$ . All variables in the  $t_c$  model are experimentally accessible and measured, and this captures relatively well the timescales observed throughout the experiments. Using non-dimensional analysis, we collapse all sedimentation front data onto a single master line that captures both bacteria concentration regimes. A phenomenological model is proposed that describes the height of the sedimentation front for a range of  $\phi_b$ . The solution of this model captures relatively well the height of the sedimentation front of the passive particles at different bacterial concentrations. In summary, micro particle-bacteria interactions are quantifiable a-priori which enables predictions of macro sedimentation rates. Further study on this field with different colloid concentrations and swimmer actuation modes (pusher vs puller) would presumably shed light on how the fundamental hydrodynamic interactions between the passive particles and active bacteria underlay the dynamics of our system and be generalized to others.

## Conflicts of interest

There are no conflicts to declare.

## Acknowledgements

We thank R. Ran, C. Kammer, and A. Patteson for fruitful discussions. B. Maldonado, and P. E. Arratia acknowledge support by the National Science Foundation grant DMR-1709763.

## Notes and references

- [1] M. Schallenberg and J. Kalff, *Ecology*, 1993, **74**, 919–934.
- [2] L. Zhang, D. Tu, X. Li, W. Lu and J. Li, *BMC Microbiology*, 2020, **20**, 254.
- [3] A. A. Roberto, J. B. Van Gray and L. G. Leff, *Water Research*, 2018, **134**, 353–369.
- [4] K. H. Nealson, *Annual Review of Earth and Planetary Sciences*, 1997, **25**, 403–434.
- [5] G. J. Herndl and T. Reinthaler, *Nature Geoscience*, 2013, **6**, 718–724.
- [6] R. F. Vaccaro, M. P. Briggs, L. Carey and B. H. Ketchum, *American Journal of Public Health*, 1257–1266, **40**, 10.
- [7] P. Tréguer and P. Pondaven, *Nature*, 2000, **406**, 358.
- [8] J. Sarmiento and J. Toggweiler, *Nature*, 1984, **308**, 621–624.
- [9] T. a. Kiørboe, *A Mechanistic Approach to Plankton Ecology* /, Princeton University Press., Princeton, NJ ;, 2008.
- [10] S. Giorgi, B. A. H. Reitsma, H. J. F. van Fulpen, R. W. P. Berg and M. Bechger, *Water Science and Technology*, 2018, **78**, 1597–1602.

- [11] J. T. Boock, A. J. E. Freedman, G. A. Tompsett, S. K. Muse, A. J. Allen, L. A. Jackson, B. Castro-Dominguez, M. T. Timko, K. L. J. Prather and J. R. Thompson, *Nature Communications*, 2019, **10**, 587.
- [12] J. A. Vázquez, A. I. Durán, A. Menduñía and M. Nogueira, *Biomolecules*, 2020, **10**, –.
- [13] J. Hugenholtz and E. J. Smid, *Current Opinion in Biotechnology*, 2002, **13**, 497–507.
- [14] L. Boutilier, R. Jamieson, R. Gordon, C. Lake and W. Hart, *Water Research*, 2009, **43**, 4370–4380.
- [15] R. H. Davis and A. Acrivos, *Annual Review of Fluid Mechanics*, 1985, **17**, 91–118.
- [16] E. Guazzelli and J. Hinch, *Annual Review of Fluid Mechanics*, 2011, **43**, 97–116.
- [17] R. Piazza, *Reports on Progress in Physics*, 2014, **77**, 056602.
- [18] R. Piazza, S. Buzzaccaro and E. Secchi, *Journal of Physics: Condensed Matter*, 2012, **24**, 284109.
- [19] T. A. Brzinski and D. J. Durian, *Phys. Rev. Fluids*, 2018, **3**, 124303.
- [20] E. Guazzelli and J. F. Morris, *A physical introduction to suspension dynamics*, Cambridge University Press, 2011, vol. 45.
- [21] J. Palacci, C. Cottin-Bizonne, C. Ybert and L. Bocquet, *Physical Review Letters*, 2010, **105**, 088304.
- [22] S. Hermann and M. Schmidt, *Soft Matter*, 2018, **14**, 1614–1621.
- [23] J. Singh, A. Patteson, B. Torres Maldonado, P. K. Purohit and P. E. Arratia, *Soft Matter*, 2021, –.
- [24] F. Ginot, I. Theurkauff, D. Levis, C. Ybert, L. Bocquet, L. Berthier and C. Cottin-Bizonne, *Physical Review X*, 2015, **5**, 011004.
- [25] J. Vachier and M. G. Mazza, *The European Physical Journal E*, 2019, **42**, 11.
- [26] F. Ginot, A. Solon, Y. Kafri, C. Ybert, J. Tailleur and C. Cottin-Bizonne, *New Journal of Physics*, 2018, **20**, 115001.
- [27] M. C. Marchetti, J. F. Joanny, S. Ramaswamy, T. B. Liverpool, J. Prost, M. Rao and R. A. Simha, *Rev. Mod. Phys.*, 2013, **85**, 1143–1189.
- [28] H. M. López, J. Gachelin, C. Douarche, H. Auradou and E. Clément, *Physical Review Letters*, 2015, **115**, 028301.
- [29] J. Gachelin, G. Miño, H. Berthet, A. Lindner, A. Rousselet and E. Clément, *Physical Review Letters*, 2013, **110**, 268103.
- [30] X.-L. Wu and A. Libchaber, *Physical Review Letters*, 2000, **84**, 3017–3020.
- [31] D. T. N. Chen, A. W. C. Lau, L. A. Hough, M. F. Islam, M. Goulian, T. C. Lubensky and A. G. Yodh, *Physical Review Letters*, 2007, **99**, 148302.
- [32] G. Miño, T. E. Mallouk, T. Darnige, M. Hoyos, J. Dauchet, J. Dunstan, R. Soto, Y. Wang, A. Rousselet and E. Clément, *Physical Review Letters*, 2011, **106**, 048102.
- [33] A. Jepson, V. A. Martinez, J. Schwarz-Linek, A. Morozov and W. C. K. Poon, *Physical Review E*, 2013, **88**, 041002.
- [34] A. E. Patteson, A. Gopinath, P. K. Purohit and P. E. Arratia, *Soft Matter*, 2016, **12**, 2365–2372.
- [35] J. Tailleur and M. Cates, *Phys. Rev. Lett.*, 2008, **100**, 218103.
- [36] J. Tailleur and M. Cates, *Euro. Phys. Lett.*, 2009, **86**, 60002.
- [37] R. W. Nash, R. Adhikari, J. Tailleur and M. E. Cates, *Phys. Rev. Lett.*, 2010, **104**, 258101.
- [38] Z. Wang, H. Y. Chen, Y. J. Sheng and H. K. Tsao, *Soft Matter*, 2014, **10**, 3209–3217.
- [39] J. Schwarz-Linek, C. Valeriani, A. Gacciuto, M. E. Cates, D. Marenduzzo, A. N. Morozov and W. C. K. Poon, *Proc. Natl. Acad. Sci.*, 2012, **109**, 4052–4057.
- [40] R. Jeanneret, D. O. Pushkin, V. Kantsler and M. Polin, *Nature Comm.*, 2016, **7**, 12518.
- [41] J. Richardson and W. Zaki, *Chemical Engineering Science*, 1954, **3**, 65–73.
- [42] T. V. Kasyap, D. L. Koch and M. Wu, *Physics of Fluids*, 2014, **26**, 081901.
- [43] H. C. Berg, *E. coli in Motion*, Springer Science & Business Media, 2008.